Available online at www.sciencedirect.com
SCIENCE DIRECT
Polymer 46 (2005) 4397–4404
polymer
www.elsevier.com/locate/polymer

# Deformation of glassy polycarbonate and polystyrene: the influence of chemical structure and local environment

Sergei Shenogin[a,b], Rahmi Ozisik[a,b,*]

[a]Rensselaer Nanotechnology Center, Rensselaer Polytechnic Institute, Troy, NY 12180, USA
[b]Department of Materials Science and Engineering, Rensselaer Polytechnic Institute, Troy, NY 12180, USA

Available online 2 April 2005

**Abstract**

Understanding the mechanism of deformation is very important in various applications. Although the stress–strain behavior of crystals and glasses are similar, the mechanism of deformation is very different. We used molecular dynamics to study polycarbonate and polystyrene under constant external loads. The results indicate that high atomic/segmental mobility and low local density enable the formation (nucleation) of highly deformed regions that grow to form plastic defects, and the effect of chemical structure was found to dominate the deformation mechanism


*Keywords:* Deformation; Glassy polymer; Molecular dynamics

## 1. Introduction

The properties of ordered and disordered materials are similar at the continuum scale but vary a great deal at the atomistic scale. There are various problems that need further study in the physics of disordered materials involving structural, thermodynamic, mechanical properties. One main difficulty in the study of disordered systems is due to the fact that methods of solid state physics such as dislocation theory or dynamic analysis [1] developed for ordered state are not applicable to disordered materials. The study of disordered materials requires a different approach where the localization of the macroscopic properties should be considered [2–4].

The deformation of ordered systems, such as crystals, has been studied extensively [5,6]. The dislocation theories of plasticity give reliable explanations for the macroscopic deformation behavior of crystals (yielding, strain softening, and hardening), and for structural changes caused by deformation (development of shear bands, etc.) [1]. The macroscopic plastic behavior of polymer glasses is very similar to that of crystals at the continuum scale: deformed polymer glasses exhibit yielding, strain softening, and hardening processes. However, recent experimental results obtained in various experiments (deformation calorimetric studies, residual strain recovery rate measurements, thermally stimulated creep, differential scanning calorimetry) suggest that the atomic scale mechanism of plastic flow in glasses and crystalline materials is very different. It was found that unlike crystals, the nucleation and initial development of plastic deformation in glasses is not accompanied by heat release [7] and that all external work is stored as internal energy in localized plastic structural defects [8–15]. The difference between the dislocations in crystals and plastic defects in glasses is in the high localization of the plastic defects. These plastic defects in glasses were termed plastic shear transformations (PSTs). Once PSTs are initiated, they cannot grow or propagate through the disordered structure, which means that they have higher localization then dislocation loops in crystals. The distribution of linear plastic defects in crystals is replaced with the distribution of localized plastic defects in the glass. A number of theories were suggested with different assumptions about the geometry of local plastic defects, their internal energy, and their interaction energy [16]. With the use of fitting parameters, most of these theories can satisfactorily describe the experimental macroscopic deformation of polymer glasses. However, modern experimental techniques cannot provide information about

* Corresponding author. Address: Rensselaer Polytechnic Institute, MRC-205, Troy, NY 12180, USA.
*E-mail address:* ozisik@rpi.edu (R. Ozisik).

0032-3861/$ - see front matter © 2005 Elsevier Ltd. All rights reserved.
doi:10.1016/j.polymer.2005.03.015

the possible structure of plastic defects in glasses. Standard structural methods such as electron microscopy, atomic force microscopy, or X-ray analysis cannot detect changes caused by plastic deformation in glassy polymers. These methods are essentially useless in the chaos of the glassy structure. More indirect methods were used to measure the changes in free volume distribution (i.e., positron annihilation) [17–20] or vibrational spectrum (i.e., Raman spectroscopy) due to plastic deformation of polymer glasses. These valuable results, however, cannot tell much about the micro mechanism of plasticity in glasses, i.e. what kind of plastic defects are produced by deformation.

Atomistic scale computer simulations are very promising in the study of disordered structures. Mott et al. [21] performed explicit atom simulations on atactic polypropylene. A small extensional strain step is applied to a minimized starting structure with three-dimensional periodicity. Subsequent minimization causes the system to search for a new minimum energy conformation, and when this is done repeatedly, large deformations can be simulated at infinitesimally small strain rates. Mott's results revealed "jumps" in the stress–strain curve that correspond to excessive rearrangement of the entire structure. The stress–strain behavior was found to be reversible (elastic) before the jumps, but irreversible (plastic) after the jumps took place. It was also observed that the plastic events corresponded to global rearrangement of the chains and were not restricted to a local region or a single chain. Argon et al. [22] calculated the region going through plastic deformation to be on the order of $\sim$10 nm. Simulations performed using Monte Carlo [23,24] or Molecular Dynamics [25] techniques often give reasonable qualitative results for plastic deformation behavior of model glasses. Assuming that the correct force field was selected, the yielding at the correct level of stress and strain hardening at higher deformation can be simulated and experimental stress–strain diagrams can be reproduced [25,26]. However, direct atomic-level simulations of plastic deformation in polymer glasses could not reproduce the correct energy storage for the deformed structure and thermally stimulated recovery of deformation. A probable reason is that even with up-to-date computers, the size of the amorphous structure that may be simulated is limited to nanometers. As a result, a long-range interaction between plastic defects is excluded from consideration, and therefore, the typical deformational behavior of simulated structure is very different from the reality.

Another important problem is the long relaxation times inherent to polymers. The time scales attainable by simulations are extremely small. In addition, the rates at which the deformation can be imposed in computer experiments are much higher than those in real life experiments. High sensitivity of deformation behavior of polymer glasses to the variation of strain rate and temperature suggests typical time scales for deformation molecular relaxation processes in the order of 1–100 s. Obviously, these large-scale slow deformation processes cannot be simulated by means of explicit computer simulations.

In this study, we will investigate local changes in glassy structures of polycarbonate and polystyrene upon small deformation. The following section will explain the simulation method, followed by results and discussion. We will summarize our findings in the conclusions section.

## 2. Simulation setup

Atomistic-level simulations of glassy polymer structures were performed using a recently developed in-house code, named Macromolecular Reality [27,28], which is similar to the Discover module found in Accelrys, Inc. products. Macromolecular Reality contains CFF91 [29], PCFF [30], PCFF with second order cross-terms, and our own specialized force fields. CFF91 and PCFF are second generation force fields, derived based on ab initio models. CFF91 was parameterized against a wide range of experimental observables for organic compounds containing H, C, N, O, S, P, halogen atoms and ions, alkali metal cations, and several biochemically important divalent metal cations. PCFF is based on CFF91, extended so as to have a broad coverage of organic polymers, metals, and zeolites. We are using the PCFF force field developed by Ulrich W. Suter and his co-workers [31]. Macromolecular Reality also includes a graphical user interface created in our laboratory (called XenoView) and uses common file formats.

Glassy polymer structures were created using a method first proposed by Suter and collaborators [32] (the software code is called PolyPack). It consists of a heuristic search algorithm in the space of torsion angles, which automatically delivers the correct conformational statistics of the chains. In our simulations, we used the experimental density as an initial condition for the PolyPack calculation, therefore requiring the initial structures to be packed properly. The performance and efficiency of this method have been previously verified for polyethylene and polystyrene [32]. Four polycarbonate and three polystyrene initial structures were created and studied. This improves the reliability of the results obtained from simulations.

All atoms were explicitly defined. Three-dimensional periodic boundary conditions were imposed during simulations. The typical computational cell size was about 3–4 nm, which assumes 2500–6000 atoms. A sample polycarbonate structure is shown in Fig. 3 that contains three molecules with 827 atoms each, with cell size about 3 nm, and the polystyrene structure shown in Fig. 4 contains 9 molecules with 642 atoms each in cubic cell with size about 4 nm.

Constant temperature isostress ensemble [33] was used in all simulations. Temperature was set to 298 K in all simulations by means of a thermostat with soft velocity rescaling method [34]. A 0.5 fs time step was used in all

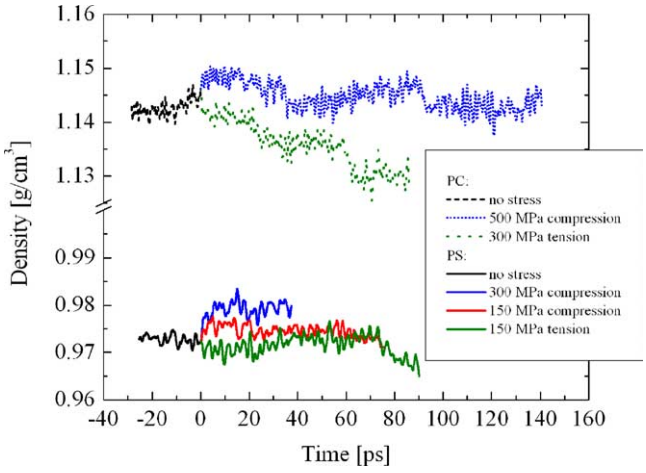


Fig. 1. The fluctuations in (global) density of polycarbonate and polystyrene before deformation, and after tensile or compressive load was applied at time $t=0$.

simulations. Each system was further equilibrated under atmospheric pressure for 30–40 ps before the application of external load. The experimental density of polycarbonate and polystyrene was recovered during the equilibration (Fig. 1). At standard temperature and pressure conditions, structures remained stable for up to 200 ps of simulation.

The nearest neighbors of each atom were defined using Voronoi polyhedra analysis. The deformation was achieved by applying constant external loads (uniaxial tension, uniaxial compression, and hydrostatic compression). The applied stresses were always kept below the yield stress value in order to achieve global strains of 1–5%. This also ensured that most atoms do not experience a change in their nearest neighbors, and that the structure can be stable under

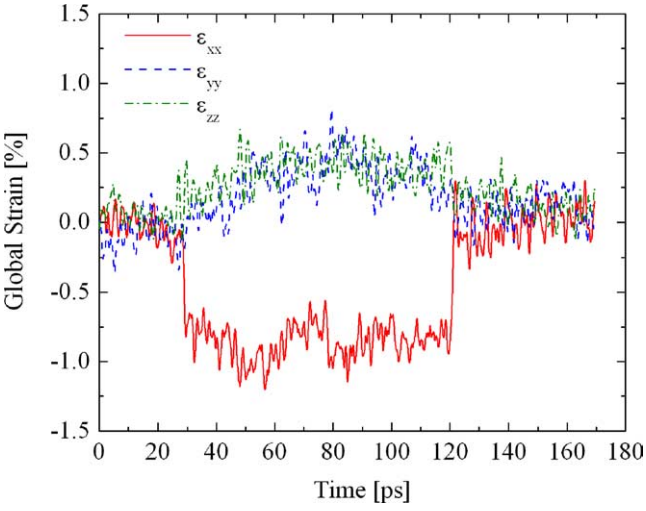


Fig. 2. The fluctuations in global strains experienced by polycarbonate under uniaxial compression. A constant 500 MPa load was applied along the $x$-axis. The simulation box experienced a global strain of 1.0% but when the external load was removed, the simulation box recovered its original size.

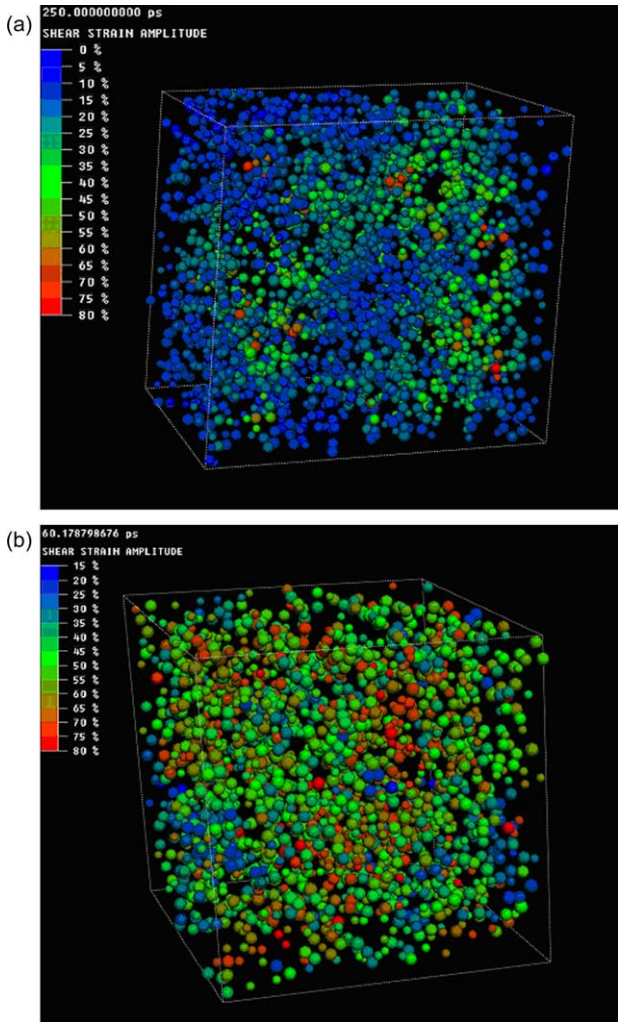


Fig. 3. Distribution of local shear strain in polycarbonate under (a) tensile deformation and (b) hydrostatic compression. Atoms are colored according to the shear strain values that their Voronoi volume is experiencing.

stress for 20 ps required for time averaging in the deformed stage.

From the displacement of nearest neighbors in the deformed state, local strain tensor, $\|\varepsilon\|$, was obtained for each atom's Voronoi volume from the minimization of the following equation:

$$\Delta R^2 = \frac{1}{N}\sum_{i=1}^{N}(\Delta\vec{r}_{\mathrm{def},i} - \|\varepsilon\|\cdot\vec{r}_{\mathrm{o},i})^2 \quad (1)$$

where $N$ is the number of nearest neighbors, $\boldsymbol{r}_{\mathrm{def},i}$ is the actual relative displacement of each neighbor after deformation, $\boldsymbol{r}_{\mathrm{o},i}$ is the relative position of each nearest neighbor, $\Delta R^2$ is the accuracy of local strain field with respect to the constant tensor $\|\varepsilon\|$ with six independent components, and the summation is performed over all nearest neighbors. Finding the minimum of Eq. (1) requires the solution of a set of six linear equations, giving all six independent components of the local strain tensor $\|\varepsilon\|$. An alternative

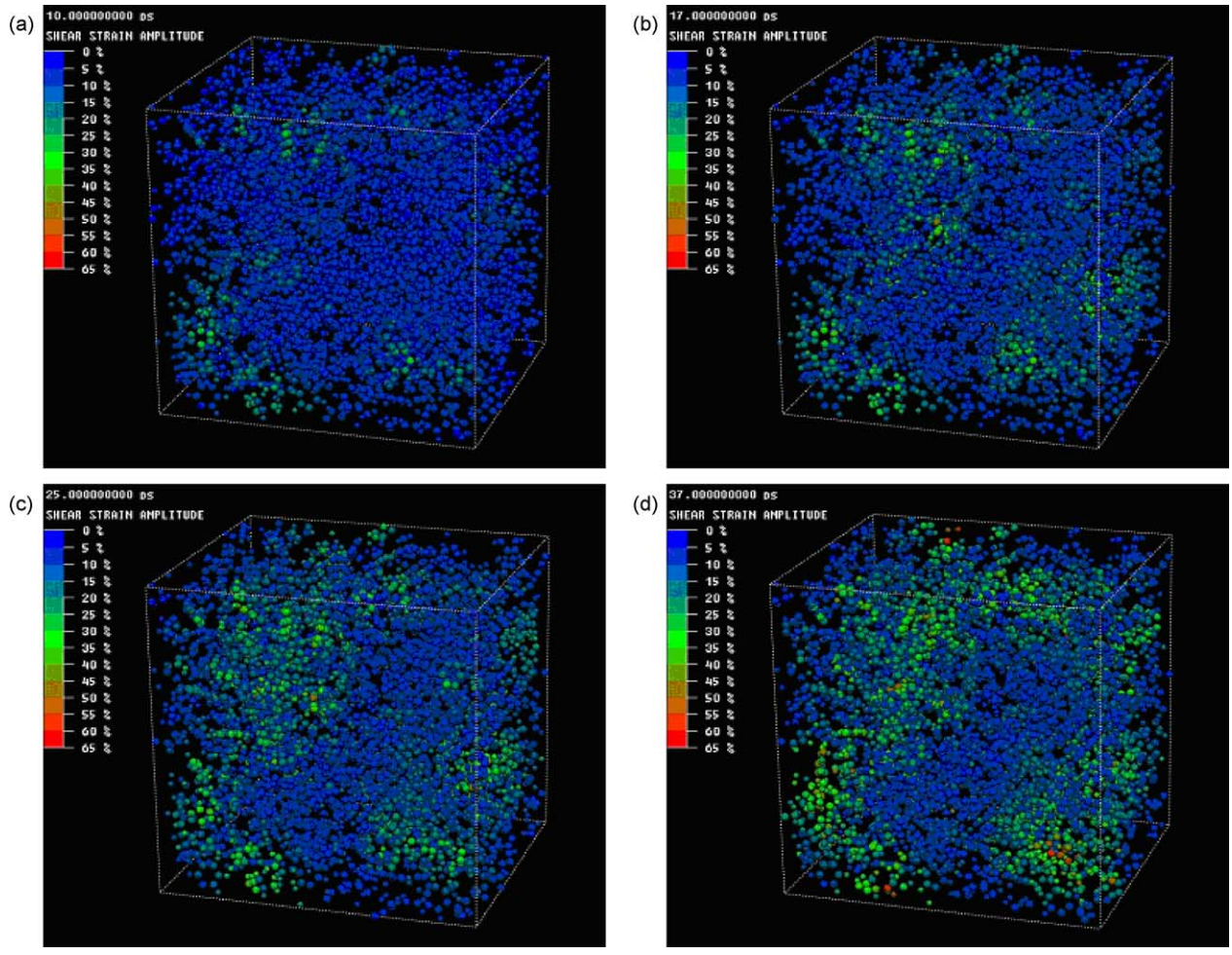


Fig. 4. Nucleation and growth of inelastic shear strain in polystyrene at (a) 0.8%, (b) 1.5%, (c) 2.0% and (d) 2.4% global strain.

procedure, suggested by Mott et al. [35] assumes space-averaging between the displacement gradients of individual neighboring atoms:

$$\varepsilon_{ij} = \frac{1}{F_\Sigma} \sum_{\text{tetrahedra}} \frac{f_n}{2} \left[ \frac{\Delta r_{\text{def}_i}}{\Delta r_{\text{O}_j}} + \frac{\Delta r_{\text{def}_j}}{\Delta r_{\text{O}_i}} \right] \tag{2}$$

where $f_n$ is volume fraction of the Delaunay tetrahedron formed by a central atom and three of its nearest neighbors, and $\Delta r_{\text{O}}$ and $\Delta r_{\text{def}}$ are offsets and relative displacements of these neighbors, respectively. However, some neighboring atoms often have very small offsets in a given direction (i.e. both $\Delta r_{\text{O}}$ and $\Delta r_{\text{def}}$ values are small), which results in large statistical errors for the ratio $\Delta r_{\text{def}}/\Delta r_{\text{O}}$ and large scattering for the components of the local strain tensor $\|\varepsilon\|$ defined by Eq. (2). Therefore, definition of local strain tensor through Eq. (1) was used in this paper. We calculated two scalar invariants of tensor $\|\varepsilon\|$: local hydrostatic strain (Eq. (3)) and local shear strain (Eq. (4)):

$$\varepsilon_{\text{hydro}} = \frac{1}{3} \delta_{ij} \varepsilon_{ij} \tag{3}$$

$$\varepsilon^2_{\text{shear}} = \frac{2}{3} (\varepsilon_{ij} - \delta_{ij} \varepsilon_{\text{hydro}})^2 \tag{4}$$

In this simulation, small loads were applied to the simulation box and atomic strains were calculated according to Eq. (1), but it is also possible to apply small deformations to the simulation box and calculate atomic stresses [36]. As far as we know, there is no advantage of one method over the other.

In this study, spatial distribution of local strain tensor $\|\varepsilon\|$ components were analyzed for each deformation mode. The goal is to find correlations between local packing and local shear strain value, and detect the localization of shear strain that can be considered as plastic defect.

## 3. Results and discussion

The simulations on polycarbonate and polystyrene were performed using the Macromolecular Reality molecular dynamics code. Various parameters were collected during the simulations and we are going to present some of them that are relevant to deformation. During the simulations, we

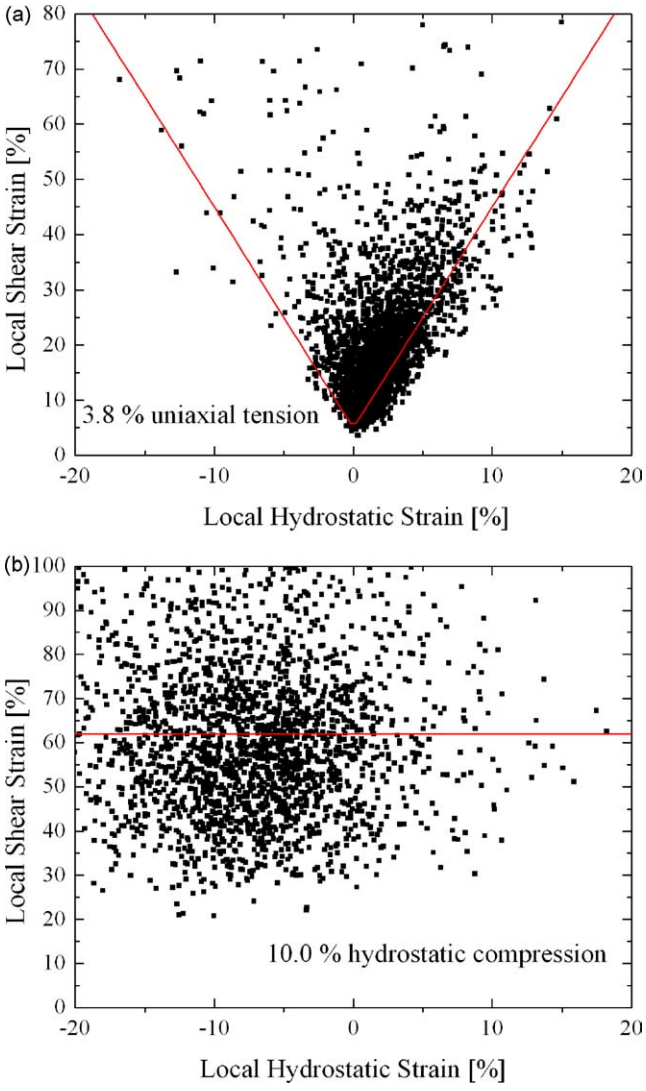


Fig. 5. Local shear strain experienced by the Voronoi volume of each atom vs. the local hydrostatic strain for polycarbonate under (a) uniaxial tension and (b) hydrostatic compression.

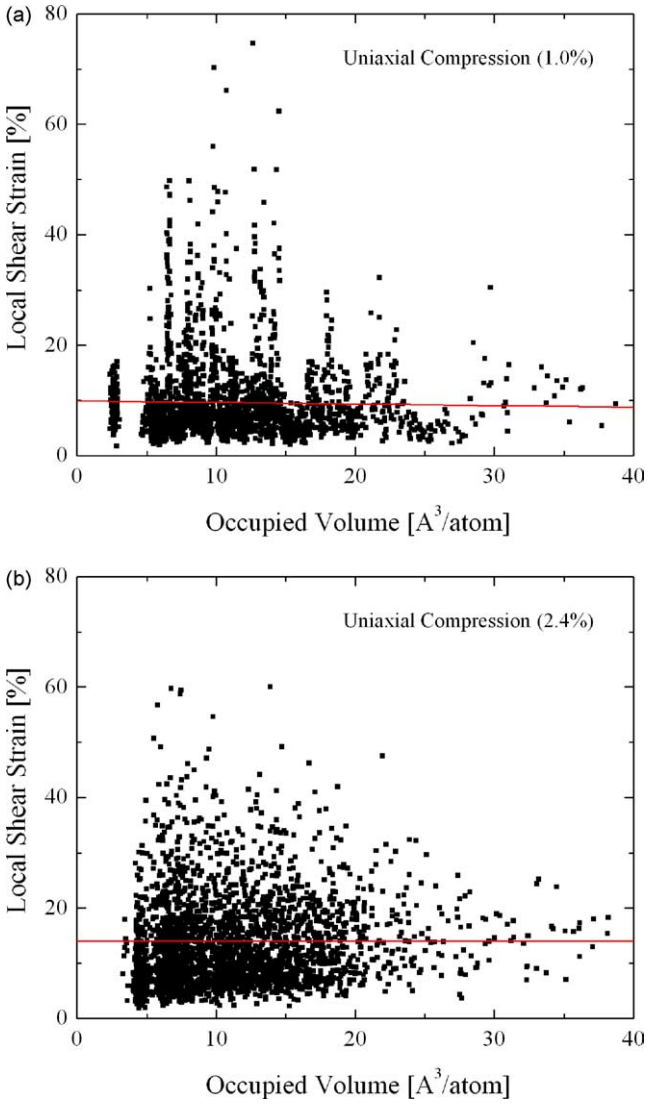


Fig. 6. Local shear strain experienced by the Voronoi volume of each atom vs. the initial occupied volume under uniaxial compression for (a) polycarbonate (1.0% global strain) and (b) polystyrene (2.4% global strain).

followed the density of the simulation box as a function of time (see Fig. 1). Two observations can be made from the density data: (i) the densities of both polycarbonate and polystyrene fluctuated around their experimentally accepted values, and (ii) after an initial density jump (which lasted 5–7 ps) associated with pure elasticity, the global density changes only slightly with the deformation. This suggests that the initiation of uniaxial inelastic deformation, in contrast to the elastic one, does not cause dilatation in the structure. However, at high levels of tensile strain, some tendency to density decrease was observed (see Fig. 1). Fig. 2 shows the change in global strains under small compressive deformation as a function of time. The system deformed instantaneously when the external load was applied. The strains in the other two axes also changed as a result of deformation. All three principal strains relaxed when the external load was removed. The global strains that are reported from now on are averages of the strain fluctuations while the external load is being applied.

During our simulations, we tried to reach global strains that are less than 10% (generally less than 4%). Although, the global strain values were kept very low, the local strains calculated according to Eq. (1) were very high. Figs. 3 and 4 show the local shear strains for polycarbonate and polystyrene. Atoms in these pictures are color coded according to the shear strains that their Voronoi volume experienced. We picked snapshots that show a limited number of regions with high shear strains (as indicated by the red regions) for easier view. These pictures also indicate that there is a sharp contrast between uniaxial and hydrostatic loads. The deformed regions remained localized around these initial “hot spots” when uniaxial loads were applied (Figs. 3(a) and 4). Distribution of local shear strain in polystyrene as a function of time is shown in Fig. 4. It is

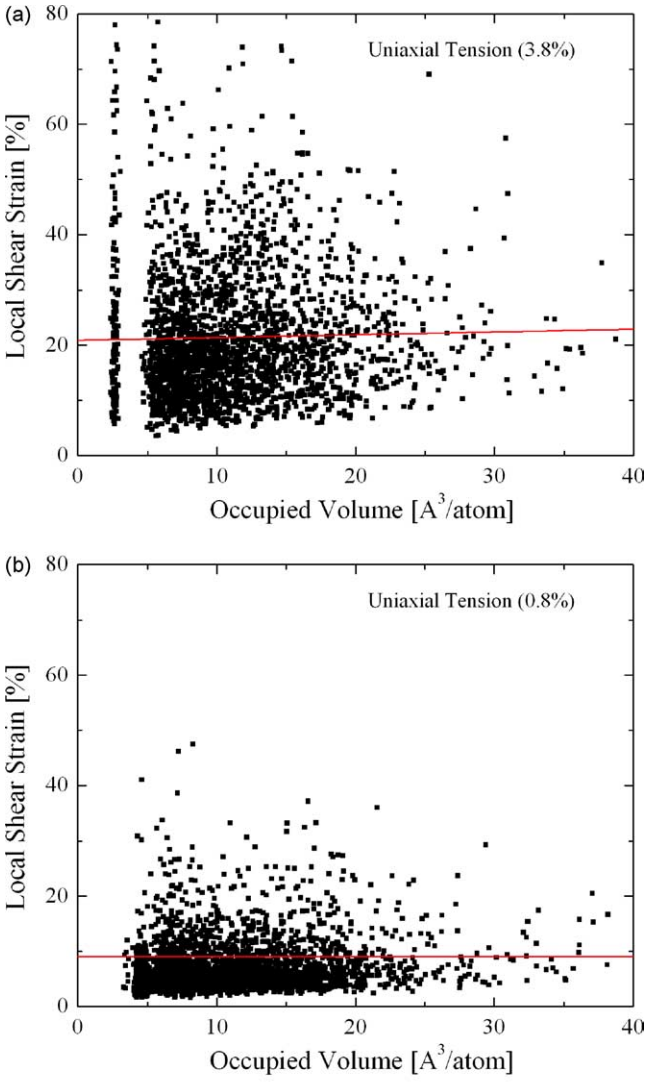


Fig. 7. Local shear strain experienced by the Voronoi volume of each atom vs. the initial occupied volume under uniaxial tension for (a) polycarbonate (3.8% global strain) and (b) polystyrene (0.8% global strain).

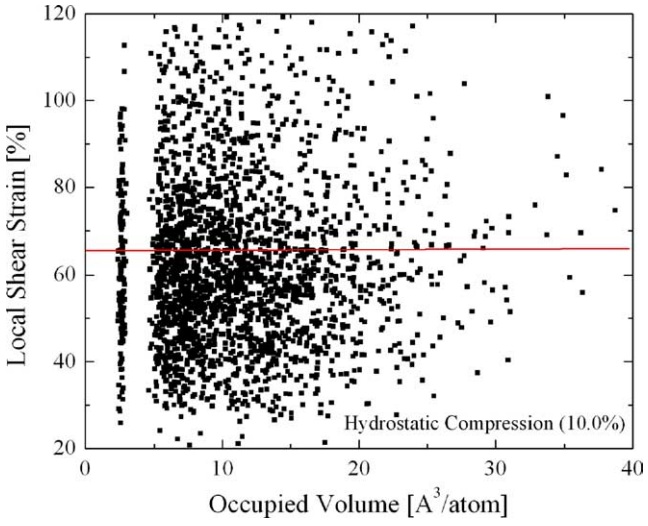


Fig. 8. Local shear strain experienced by the Voronoi volume of each atom vs. the initial occupied volume for polycarbonate under 10% hydrostatic compression.

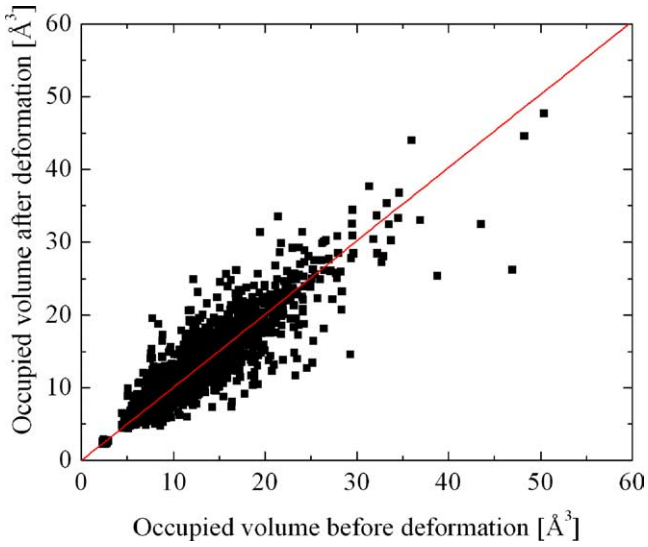


Fig. 9. The correlation between the Voronoi volume of each atom before and after the application of external load for polycarbonate. The global strain is 3.8% under uniaxial tension.

obvious that upon application of external load, certain regions that deformed initially remained the focus point of deformation regions, and "growth" of deformation took place around these initial hot spots. On the other hand, the development (initiation) and the distribution of the high shear strain regions under hydrostatic loads were diffuse-no localization was observed (Fig. 3 (b)). The correlation between the local shear strains and the local hydrostatic strains are shown in Fig. 5, where each atom is represented with a point. When uniaxial loads were applied, localization of local shear strains was observed (Fig. 5 (a)). On the other hand, when a hydrostatic external load was applied, there was no correlation between the local hydrostatic and local shear strains (Fig. 5 (b)). Similar results were obtained for polystyrene.

Figs. 6–8 show the correlation between local shear strains and the volume occupied by the atoms (Voronoi volume). In all deformation modes, the atoms experienced a wide range of local shear strains within their Voronoi volume. Although the data showed a lot of scatter, one can clearly see that there is no significant correlation between shear strain and occupied volume of the atoms. In another work by Capaldi et al. [25] no correlation between local density and deformation induced mobility was observed. Our results indicate that the variation of local density (local packing) does not affect the deformation mechanism very strongly. We also looked at our data to see if there was a correlation between the occupied volume before and after deformation for polycarbonate. The global strain in this example is 3.85% under uniaxial tension. The solid line in

Fig. 9 is a linear least squares fit to the data and has a slope of 1.006. This suggests that overall there is a very small change in the occupied volume of each atom upon deformation. The spread of the data along the $x=y$ line also suggests that there is almost an equal probability for an atom's volume to increase or decrease upon deformation. It is probable that the local environment that is defined by the Voronoi volume is either too small to capture an effect (we need to enlarge the environment), or there really is no effect of local environment in the deformation process. This would suggest that it is the inherent chemical structure that plays a major role in the initiation of deformation-it is the flexibility of the atom/segment that influences the deformation process, at least in the early stages of deformation.

The mobility of atoms can be deduced from their displacements. Fig. 10 shows the local shear strains vs. the displacement of atoms before the application of external load. The solid lines are linear least squares fit to the data at two different strains: 0.8 and 3.8% under uniaxial tension. The two solid lines have almost identical slopes, the only difference is a shift in the $y$-axis as a result of increased global shear strain. More important is the fact that the slopes have a positive value indicating a strong correlation between local shear strain and mobility. Clearly, the initiation of inelastic deformation process is predominantly affected by the local mobility/flexibility of segments and not by the (local) environment as explained above. These findings indicate relationship between local density, local mobility, and local shear strain in the early stages of deformation.

## 4. Conclusions

The deformation of glassy polycarbonate and polystyrene were studied using molecular dynamics with PCFF force field [31]. Voronoi tessellation was used to define the volume occupied by each atom. Our conclusions are as follows:

- The local shear strains were calculated according to a newly proposed method (Eq. (1)) for the volume occupied by each atom. According to this definition of local shear strain, the local shear strains exceeded the global shear strains substantially.
- The local shear strains were highly localized when uniaxial external loads were applied. Such localization was not observed for hydrostatic load.
- The nucleation of inelastic deformation requires high initial atomic/segmental mobility. The correlation between local density and local shear strains is very weak.
- Deformation induced mobility was found to depend on the chemical structure rather than the local packing density.

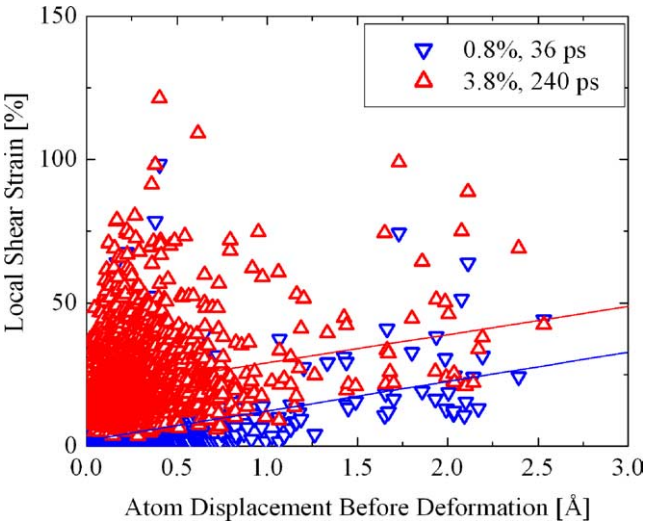


Fig. 10. Correlation between local shear strain and atom mobility. The $x$-axis shows the displacement of atoms before external stress was applied. Each point corresponds to an atom in the simulation box.

## Acknowledgements

It was a great honor for us to contribute to this special issue in honor of James E. Mark, who always inspired me (R.O.) during my studies and professional career and continues to do so even today. We would like to acknowledge the financial support provided by the Office of Naval Research (Grant number N00014-01-10732) and Rensselaer Polytechnic Institute to perform this work.

## References

[1] Nabarro FRN. Theory of crystal dislocations. Oxford: Oxford University; 1967.
[2] Zeller RC, Pohl PO. Phys Rev B 1971;4:2029.
[3] Anderson PW, Halperin BI, Varma CM. Philos Mag 1972;25:1.
[4] Phillips WA. J Low Temp Phys 1973;11:757.
[5] Peierls RE. Proc Phys Soc London A 1940;52:436.
[6] Taylor GI. Proc Roy Soc A 1934;145:362.
[7] Shenogin SV, Hoehne GWH, Oleinik EF. Thermochim Acta 2002; 391:13.
[8] Oleinik EF, Salamatina OB, Rudnev SN, Shenogin SV. Polym Sci 1993;35:1819.
[9] Gilman JJ. J Appl Phys 1973;44:675.
[10] Li JCM, Gilman JJ. J Appl Phys 1970;41:4248.
[11] Bowden PB, Raha S. Phys Mag 1974;29:149.
[12] Argon AS. In: Uhlman DR, Kreidel NJ, editors. Glass science and technology, vol. 5. New York: Academic press; 1980. p. 79.
[13] Spaepen F. Acta Met 1977;25:407.
[14] Brady TE, Yeh GSY. J Appl Phys 1971;42:4622.
[15] Falk ML, Langer JS. Phys Rev E 1998;57:7192.
[16] Langer JS, Pechenik L. Phys Rev E 2003;68:061507.
[17] Oleinik E, Shenogin S, Paramzina T, Rudnev S, Shantarovich V, Azamatova Z, et al. Polym Sci A 1998;40:1187.
[18] Shantarovich VP, Novikov YA, Suptel ZK, Oleinik EF, Boyce MC. Acta Phys Pol A 1999;95:659.

[19] Wolff J, Franz M, Broska A, Kerl R, Weinhagen M, Kohler B, et al. Intermetallics 1999;7:289.
[20] Flores KM, Suh D, Dauskardt RH, Asoka-Kumar P, Sterne PA, Howell RH. J Mater Res 2002;17:1153.
[21] Mott PH, Argon AS, Suter UW. Polym Preprints 1989;30:34.
[22] Argon AS, Bulatov VV, Mott PH, Suter UW. J Rheol 1995;39:377.
[23] Koteljanskii M. Trends Polym Sci 1997;5:192.
[24] van Workum K, de Pablo JJ. Nano Lett 2003;3:1405.
[25] Capaldi FM, Boyce MC, Rutledge GC. Polymer 2004;45:1391.
[26] Yip S, Sylvester MF, Argon AS. Comp Theor Polym Sci 2000; 10:235.
[27] See http://www.rpi.edu/(ozisik/ for more information.
[28] Shenogin S, Ozisik R. Presented at the American Physical Society Meeting, Austin, TX, March 2003; paper C1.023.
[29] Mapple JR, Hwang MJ, Stockfish TP, Dinur U, Waldman M, Ewing CS, et al. J Comput Chem 1994;15:162.
[30] Sun H. J Comput Chem 1994;15:752. Sun H. Macromolecules 1995; 28:701. Sun H, Mumby S, Hagler AT. J Am Chem Soc 1994;116: 2978.
[31] Santos S, Ph.D. Dissertation, Swiss Federal Institute of Technology (ETH), Zurich, 1998.
[32] Muller M, Nievergelt J, Santos S, Suter UW. J Chem Phys 2001;114: 9764.
[33] Parinello M, Raman A. J Chem Phys 1984;76:2662.
[34] Berendsen HJC, Postma JPM, Van Gunsteren WF, Di Nola A, Haak JR. J Chem Phys 1984;81:3684.
[35] Mott PH, Argon AS, Suter UW. J Comput Phys 1992;101:140.
[36] Theodorou DN, Suter UW. Macromolecules 1986;19:379.